CrossMark

Fe$_3$O$_4$@OA–Pd and Mo$_{10}$V$_2$@NSiO$_2$ nanoparticles: an efficient and reusable catalytic system for Heck reaction under ligand free conditions

Ezzat Rafiee[1,2] · Masoud Kahrizi[1]

Abstract This paper reports the use of a novel catalytic system composed of H$_5$PMo$_{10}$V$_2$O$_{40}$ supported on nano silica (Mo$_{10}$V$_2$@NSiO$_2$) and palladium-deposited, oleic-acid-coated Fe$_3$O$_4$ (Fe$_3$O$_4$@OA–Pd) nanoparticles, as reusable catalysts for Heck coupling reaction under ligand and base free conditions. The average particle size of catalyst was measured to be about 9 nm by transmission electron microscopy. The immobilized palladium on oleic acid coated Fe$_3$O$_4$ was found to be effective in the Heck arylation of various aryl bromides and especially less reactive aryl chlorides with styrene in the presence of heteropoly acid. This method has the advantages of high yields, elimination of ligand and base, simple methodology and easy workup. Interestingly, the novel catalytic system could be recovered in a facile manner from the reaction mixture and recycled several times without any significant loss in catalytic activity. Structural changes of recovered Mo$_{10}$V$_2$@NSiO$_2$ and Fe$_3$O$_4$@OA–Pd were investigated before reusing for the next runs. Finally, synchronized reusability of both components of our catalytic system has been investigated in the model reaction.

Keywords Heck coupling · Palladium · Oleic acid · Heterogeneous catalyst · Polyoxometalate · Nanoparticles · Magnetically recoverable

✉ Ezzat Rafiee
  Ezzat_rafiee@yahoo.com; e.rafiei@razi.ac.ir

1   Department of Inorganic Chemistry, Faculty of Chemistry, Razi University,
    67149 Kermanshah, Iran

2   Institute of Nano Science and Nano Technology, Razi University, 67149 Kermanshah, Iran

Introduction

Palladium-catalyzed cross-coupling of aryl halides with olefins, known as Heck coupling, has contributed greatly to the straightforward and facile construction of carbon–carbon bonds [1–10]. This reaction is generally considered to be a homogeneous reaction most commonly catalyzed by soluble Pd(II) species with a variety of ligands, such as palladium–phosphine complexes [2], oxime palladacycles [3], palladium–salen complexes [4], and palladium–*N*-heterocyclic carbine complexes [5]. However, separation of the expensive catalyst from the product for reusing is often problematic in these homogeneous systems. Moreover, aggregation and precipitation of palladium metal in the homogeneous systems always leads to lost activity of the catalysts. Thus, heterogeneous catalysts are highly desirable, especially in large-scale synthesis, from both environmental and economic aspects. Much effort has been paid to developing heterogeneous catalytic systems that can be efficiently reused [6, 9, 10]. Original ways have been found in the elaboration of magnetic catalysts that can be easily removed using external magnets, and in the use of supported forms of catalytic systems without practical loss.

Fe_3O_4 nanoparticles as a catalyst support have been attracting more and more attention because they can be easily recovered from the reaction mixture simply by using an external magnet, thus eliminating the necessity of tedious centrifugation, filtration, or membrane separation steps [11–19].

It is noteworthy that Fe_3O_4 nanoparticles tend to aggregate, which deteriorates unique characteristic properties of nanoparticles. Coating of the nanoparticles with a suitable protective layer can decrease the degree of agglomeration and increase the stability of the palladium nanoparticles. Several molecules have been used to coat the surface of magnetic nanoparticles (MNPs). Oleic acid is particularly useful in this regard [20–23], since it is readily available and is non-toxic. In addition, oleic acid has a strong affinity for magnetite particles through interaction between its carboxy groups and iron cations on the magnetite surface. Furthermore, the twisty hydrocarbon tails of oleic acid may help to stabilize the transition metal catalysts by chains wrapping up the individual metal nanoparticles, thus preventing them from aggregating with each other.

Recently, there has been a growing number of studies done on the use of polyoxometalates (POMs) in the coupling reactions [24–27]. The unique results for coupling reactions catalyzed by palladium and POM systems encourage us to study the Heck coupling reaction catalyzed by palladium-deposited, oleic-acid-coated Fe_3O_4 (Fe_3O_4@OA–Pd) particles and $H_5PMo_{10}V_2O_{40}$ supported on nano silica ($Mo_{10}V_2$@$NSiO_2$) as an efficient, reusable and cost-effective catalytic system. The essential requirement for the Heck reaction includes a base and a ligand-stabilized active Pd species. We believe that $Mo_{10}V_2$@$NSiO_2$ is an excellent alternative for bases and a strong activator for reactants in this reaction. The use of base, ligand and non-recyclable catalysts in reported systems in the literature is not beneficial to industrial and synthetic applications. The use of high amounts of bases poses several problems, such as inability to recover, contamination of the environment, corrosion of equipment and high toxicity. Hence, there is a need for efficient, ecofriendly and recoverable alternatives to replace bases in the Heck reaction. Along this line, using heterogeneous

heteropoly acids (HPAs), which are low in toxicity, highly stable towards humidity, recyclable and air stable, can be useful. HPAs are advantageous over conventional bases as they can be easily recovered from the reaction mixture by simple filtration and can be reused without activation, thereby making the process economically and environmentally viable. This heterogeneous catalytic system can be readily recovered and reused several times without significant loss of activity.

Materials and methods

General information

All reactions were performed under an atmosphere of dry nitrogen. All chemicals used in this work were obtained from Fluka, Aldrich or Merck companies, and were used without further purification. Transmission electron microscopy (TEM) analysis was performed using the TEM microscope LEO 912AB TEM Netherland. The high-resolution transmission electron microscopy (HR-TEM) measurements were conducted using a JEOL JEM-2100F electron microscope operating at 200 kV. X-ray diffraction (XRD) measurements were performed using a Bruker AXS Company, D8ADVANCE diffractometer (Germany). Surface areas were calculated from the linear part of the BET plot. Low temperature nitrogen adsorption experiments were performed using a Quantachrome instrument (model Nova 2000) for measuring surface area and pore volume. Fourier transform infrared spectroscopy (FT-IR) spectra were recorded with KBr pellets using a Shimadzu 470 spectrophotometer. Gas chromatography was performed on a Varian CP-3800 (column: CP-Sil 8 CB fused silica capillary column). Thin layer chromatography (TLC) on precoated silica gel, fluorescent 254 nm (0.2 mm), on aluminum plates was used for monitoring the reactions. The cross-coupling products were characterized by their ^{1}H nuclear magnetic resonance (NMR) spectra.

Synthesis of oleic acid coated-Fe$_3$O$_4$ nanoparticles

The oleic acid coated-Fe$_3$O$_4$ nanoparticles were prepared by the co-precipitation method, according to a synthesis route described in our previous publication [28]. Typically, FeCl$_2$·4H$_2$O (4.3 g) and FeCl$_3$·6H$_2$O (11.6 g) were mixed with 350 mL of deionized water. The resulting solution was heated to 80 °C while stirring vigorously. Then, 20 mL of 25 % NH$_4$OH was quickly added into the solution. The resulting suspension was vigorously stirred for 5 min, and then 1 mL oleic acid was added into the suspension. After mixing for 25 min, the black precipitates were collected with the help of a magnet and washed repeatedly with deionized water and ethanol, then dried under vacuum conditions.

Synthesis of Fe$_3$O$_4$@OA–Pd catalyst

A solution of Na$_2$[PdCl$_4$] (0.011 M) in ethanol was prepared by reacting PdCl$_2$ (0.50 g, 2.82 mmol) and NaCl (0.33 g, 5.64 mmol) at room temperature. Fe@OA nanoparticles (0.5 g in 700 mL methanol) solution was held at 25 °C for 1 h and

then $Na_2[PdCl_4]$ (100 mL, 0.011 M) was added. Then 100 mL of NaOAc (5 M) was added rapidly into the solution. After that, 50 mL of methanol was added, and the product was separated by magnetic field, washed three times with ethanol and water, and dried under vacuum conditions [28].

Preparation of $Mo_{10}V_2$

$Mo_{10}V_2$ was prepared according to the following procedure: sodium metavanadate (24.4 g) was dissolved by boiling in 100 mL of water, and then mixed with 7.1 g of Na_2HPO_4 in 100 mL of water. Then this solution was cooled, 5 mL of concentrated sulfuric acid was added, and the solution developed a red color. An addition of 121.0 g of $Na_2MoO_4 \cdot 2H_2O$ dissolved in 200 mL of water was then made. While the solution was vigorously stirred, 85 mL of concentrated sulfuric acid was added slowly, and the hot solution was allowed to cool to room temperature. $Mo_{10}V_2$ was then extracted with 500 mL of diethyl ether. Evaporation of the solvent afforded a crude product that dissolved in water, concentrated to first crystal formation, and then was allowed to crystallize further. The large red crystals that formed were filtered, washed with water, and air dried [29].

Preparation of $Mo_{10}V_2@NSiO_2$

$Mo_{10}V_2@NSiO_2$ was prepared by impregnating nano silica (3.0 g) with an aqueous solution of $Mo_{10}V_2$ (with concentration depending upon the loading 40 wt% $Mo_{10}V_2$ on silica). The mixture was stirred overnight at room temperature, followed by drying using a rotary evaporator [30–32].

General procedure for the Heck coupling reaction

For the Heck coupling reaction, a reaction tube was charged with aryl halide (4 mmol), styrene (4 mmol), tetrabutylammonium bromide, TBAB (4 mmol), Fe@OA–Pd (0.02 g), $Mo_{10}V_2@NSiO_2$ (0.004 g) and 5 mL DMF, and the resulting mixture was refluxed at 120 °C under a dry nitrogen atmosphere for an appropriate time. Progress of the reaction was monitored by TLC. Upon completion of the reaction, the reaction mixture was then cooled to room temperature and Fe@OA–Pd was separated by magnet, washed with diethyl ether (2 × 10 mL) and water (2 × 10 mL), and then dried under vacuum for reusability. $Mo_{10}V_2@NSiO_2$ was also separated by filtration, and washed with diethyl ether (3 × 10 mL) and dried at 100 °C for reusing. The residual mixture was extracted by CH_2Cl_2 (3 × 20 mL), and the combined organic layer was dried over $MgSO_4$.

Results and discussion

In the present work, $Mo_{10}V_2@NSiO_2$ and $Fe_3O_4@OA–Pd$ were used as a highly efficient nano catalytic system. The catalytic activity of this two-component system was investigated in Heck reaction under base and ligand-free conditions.
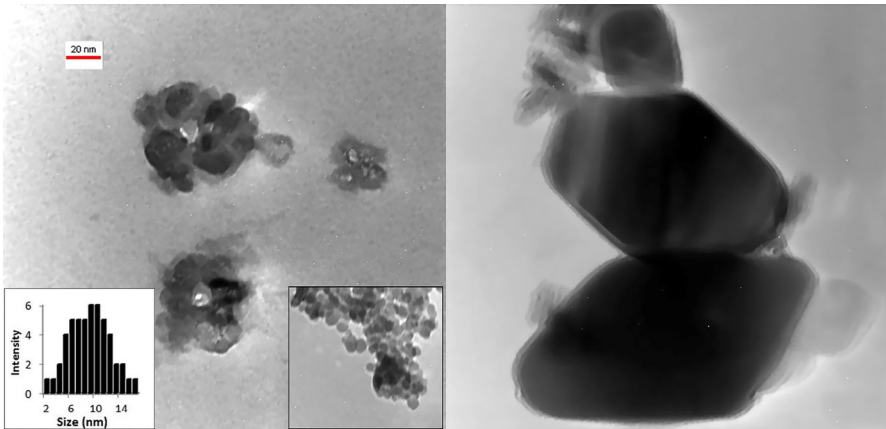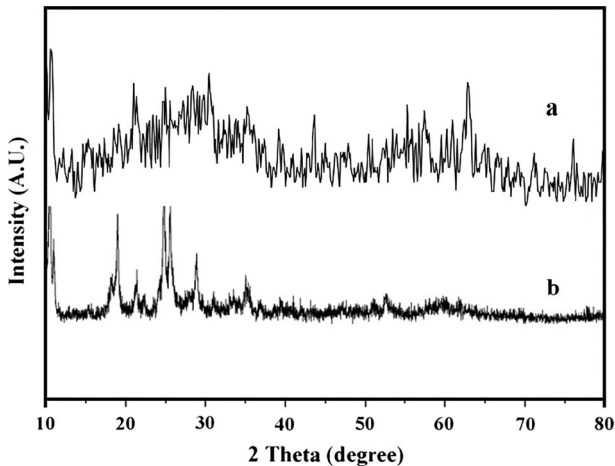
Fig. 1 TEM images and size distribution of Fe$_3$O$_4$@OA–Pd

Fig. 2 XRD patterns of *a* Mo$_{10}$V$_2$@NSiO$_2$ and *b* PMo$_{10}$V$_2$

At the beginning of our catalytic studies, the structural features of Fe$_3$O$_4$@OA–Pd catalyst were investigated using TEM techniques (Fig. 1). TEM observations indicated that Fe$_3$O$_4$@OA–Pd as a main catalyst in this catalytic system has a uniformity and spherical morphology. The average particle size of catalyst was about 9 nm. Other characterization results have been presented in our previous publication [28].

XRD patterns of Mo$_{10}$V$_2$@NSiO$_2$ and PMo$_{10}$V$_2$ are presented in Fig. 2; no obvious peak was found in the catalyst, which indicates that Mo$_{10}$V$_2$ was homogeneously dispersed in amorphous silica [33]. The nano silica and Mo$_{10}$V$_2$@NSiO$_2$ have BET surface areas of 628 and 181 m^2 g^{-1}, respectively. The surface area of catalyst decreased remarkably compared to its parent support, but

still showed very high value. The reduction in the surface area of supported catalyst may be due to the blockage of smaller pores by active species and good dispersion of $Mo_{10}V_2$.

Next, for optimization of the reaction conditions, the reaction of 1-bromonaphtalene (4 mmol) and styrene (4 mmol) at 120 °C and under ligand and base-free conditions was chosen as a model reaction (Scheme 1). First, the abilities of various catalytic systems such as $H_3PW_{12}O_{40}$ (PW), $Mo_{10}V_2$, $Pd_{2.5}PMo_{10}V_2O_{40}$ and $Mo_{10}V_2@NSiO_2$ accompanied by $Fe_3O_4@OA–Pd$ in the model reaction were investigated (Table 1). As shown in Table 1, among these catalysts, $Mo_{10}V_2$ and $Mo_{10}V_2@NSiO_2$ were found to be excellent catalysts in terms of conversion and reaction time (entries 3, 4). It may be because of this fact that $Mo_{10}V_2$ and $Mo_{10}V_2@NSiO_2$ are ideal outer-sphere electron-transfer compounds. Electron transfer between palladium species and POMs in the catalytic cycle of this reaction may help to increase the reaction efficiency. We have also studied a similar reaction
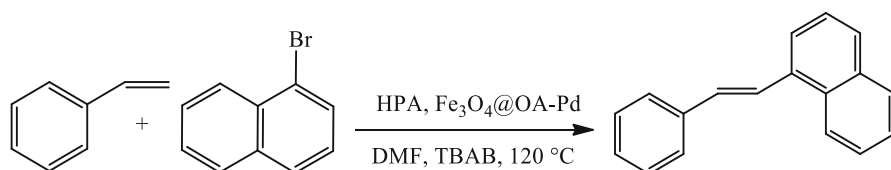
Scheme 1 Reaction of styrene and 1-bromonaphtalene as a model reaction

Table 1 Effect of the POM on the Heck coupling reaction

Entry	Catalyst		Solvent	Time (h)	Yield (%)[a]
	$Fe_3O_4@OA–Pd$ (g)	POM (g)			
1	0.01	–	DMF	24	0
2	0.01	PW (0.001)	DMF	24	32
3	0.01	$Mo_{10}V_2$ (0.001)	DMF	24	95
4	0.01	$Mo_{10}V_2@NSiO_2$ (0.004)	DMF	24	70
5	–	$Pd_{2.5}Mo_{10}V_2$ (0.001)	DMF	24	23
6	0.01	$Mo_{10}V_2@NSiO_2$ (0.004)	H_2O	24	10
7	0.01	$Mo_{10}V_2@NSiO_2$ (0.004)	Toluene	24	0
8	0.02	$Mo_{10}V_2@NSiO_2$ (0.004)	DMF	8	90
9	0.03	$Mo_{10}V_2@NSiO_2$ (0.004)	DMF	8	95
10	0.01	$Mo_{10}V_2@NSiO_2$ (0.008)	DMF	24	70
11	0.02	$Mo_{10}V_2@NSiO_2$ (0.004)	DMF	24	0[b]
12	0.02	$Mo_{10}V_2@NSiO_2$ (0.004)	DMF	24	6[c]
13	0.02	$Mo_{10}V_2@NSiO_2$ (0.004)	DMF	24	73[d]

Reaction conditions: styrene (4 mmol), 1-bromonaphtalene (4 mmol), TBAB (4 mmol) and at 120 °C

[a] Isolated yield

[b] Reaction proceeded in TBAB free conditions

[c] Reaction proceeded in room temperature condition
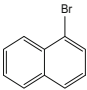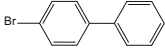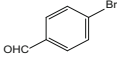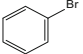
[d] Reaction proceeded at 80 °C
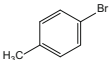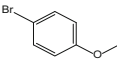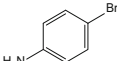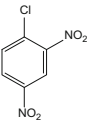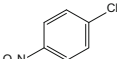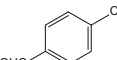
in the absence of POM. The reaction did not proceed and the starting materials remained intact after 24 h (entry 1). There is a problem here: Mo$_{10}$V$_2$ in acidic form is a homogeneous catalyst in this reaction media. The major problem, limiting the utility of homogeneously catalyzed processes, is a well-known difficulty in catalyst recovery and recycling. The recycling of POMs as catalysts is the key issue to their application. Therefore, we chose Mo$_{10}$V$_2$@NSiO$_2$ as the heterogeneous recoverable catalyst for the Heck coupling reaction.

To establishing the best reaction conditions, the effects of various solvents, such as H$_2$O, toluene and DMF, were studied (entri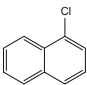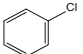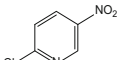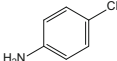es 4, 6, 7). DMF at 120 °C was found to be the choice in terms of yield and reaction time (entry 4). Next, the model reaction was carried out in the presence of different amounts of Fe$_3$O$_4$@OA–Pd as catalyst. Improvement in time of the reaction was observed as the catalyst quantity increased from 0.01 to 0.02 g. Further increase in the Fe$_3$O$_4$@OA–Pd quantity showed no improvement in the yield or reaction time (Table 1, entries 8, 9). Also, more increase in Mo$_{10}$V$_2$@NSiO$_2$ had no significant effect on the reaction time and yield (Table 1, entry 10). Having realized the optimum catalysts loading for the reaction (0.004 g of the Mo$_{10}$V$_2$@NSiO$_2$ and 0.02 g of Fe$_3$O$_4$@OA–Pd), attention turned to the evaluation of the influence of TBAB as an additive on the Heck coupling reaction. In the absence of TBAB, the reaction did not proceed even after 24 h (Table 1, entry 11), while addition of TBAB permitted us to achieve 90 % yield of the product after 8 h (Table 1, entry 8). The potential and efficiency of the tetraalkylammonium salts has been illustrated. TBAB is a phase transfer catalyst for facilitating the regeneration of the zero valent palladium catalyst. The dissociation of the hydridopalladium halide complex can be more efficient in the presence of inorganic bases [34]. Also, TBAB can act as stabilizer of palladium nanoparticles, preventing their aggregation to the bigger size particles, which are usually inactive or less active. At elevated temperature, TBAB can partially decompose to Bu$_3$N, and Bu$_3$N can facilitate the reductive elimination step. It is generally accepted that promoting the oxidative addition and reductive elimination step and prevention of palladium black formation, thereby enhancing catalyst concentration, are factors of the high catalytic activity in the presence of tetraalkylammonium salts [34–36].

Finally, the model reaction was performed at various temperatures. As shown in Table 1, with reduction of the temperature from 120 °C to room temperature, the yield decreased from 90 to 6 % (Table 1, entries 12, 13). These results demonstrated that the reaction temperature had a significant effect on the reaction progress, and further experiments were carried out at 120 °C. Therefore, 0.004 g of the Mo$_{10}$V$_2$@NSiO$_2$ and 0.02 g of Fe$_3$O$_4$@OA–Pd at 120 °C in the presence of TBAB were chosen as the optimum condition of catalytic system for further reactions.

Using the optimized reaction conditions, we explored the general applicability of Fe$_3$O$_4$@OA–Pd and Mo$_{10}$V$_2$@NSiO$_2$ as a catalytic system with styrene and other aryl halides containing electron withdrawing or donating substituents, and the results are tabulated in Table 2. It should be noted that this catalytic system showed high selectivity for the trans-configured products in all cases, and no cis/gem olefin products were observed. Among the various substituted aryl bromides, both deactivated (electron-rich) and activated (electron-poor) examples were converted efficiently to the desired products in good to excellent yields (entries 1–7). Aryl

Table 2 Heck reaction of various aryl halides with styrene

Entry	Aryl halide	Time (h)	Yield (%)[b]
1		8	90
2		8	86
3		12	91
4		12	82
5		12	83
6		12	72
7		24	71
8		9	93
9		12	91
10		12	78
11		12	86
12		12	79
13		24	91
14		24	40

Reaction conditions: styrene (4 mmol), aryl halide (4 mmol), TBAB (4 mmol) at 120 °C

[a] Isolated yield. All products were characterized by comparing their ^{1}H-NMR data with authentic samples

bromides containing electron-withdrawing functional groups give higher yields with lower reaction times compared to those containing electron-donating functional groups. As expected, aryl bromides were more reactive than aryl chlorides, and the substituent effects in the aryl bromides appeared to be less significant than in the aryl chlorides (Table 2, entries 3, 7 and 10, 14). As shown in Table 2, activated aryl chlorides such as 2,4-dinitrochlorobenzene, 4-nitrochlorobenzene and 4-chloroben-zaldehyde underwent the Heck reaction with styrene under similar conditions to afford the corresponding product in excellent yield (entries 8–10), whereas deactivated aryl chlorides such as 4-chloroaniline gave 40 % yield (entry 14). It is noteworthy that this catalytic system also had the ability to couple styrene with sterically hindered substrates such as 1-bromonaphthalene, 4-bromobiphenyl, 1-chloronaphthalene and 2, 4-dinitrochlorobenzene in reasonable yields (Table 2, entries 1, 2, 8, 11).

In recent years, reusable solid acid catalysts have attracted a great deal of interest. Since most of the catalysts are expensive and contaminate the environment, the development of efficient methods for recovery and reusing of the catalyst is very important. Thus, investigations of the factors that affect the reusability of the catalyst have especially profound importance. We decided to investigate the structural changes of recovered Mo$_{10}$V$_2$@NSiO$_2$ and Fe$_3$O$_4$@OA–Pd before reusing for the next runs. In order to determine the changes of both components of our catalytic system, Mo$_{10}$V$_2$@NSiO$_2$ and Fe$_3$O$_4$@OA–Pd were separated from the model reaction, and their structural changes were determined by FT-IR technique. As shown in FT-IR spectra of the fresh and recovered Fe$_3$O$_4$@OA–Pd (Fig. 3), it seems that the reaction media and temperature did not effect the structure of Fe$_3$O$_4$@OA–Pd. The broad band near 3400–3500 cm^{-1} in Fig. 3 refers to the OH stretching vibration associated with absorbed water molecule. Two bands at around 2860–2930 cm^{-1} were attributed to the asymmetric and symmetric stretching of CH$_2$ groups of oleic acid, respectively. The peak at about 1625 cm^{-1} exhibited the presence of the C=C stretching vibration. From Fig. 3, it is clear that the band at 1710 cm^{-1}, which was assigned to the stretching vibration of C=O in oleic acid, is absent in the spectrum of Fe$_3$O$_4$@OA particles. Meanwhile, two new bands at about 1415 and 1570 cm^{-1} appeared, and are characteristic of the asymmetric –(COO$^-$) and the symmetric –(COO$^-$) stretch vibration bands, respectively. These results could be explained by the fact that oleic acid was chemically absorbed onto the surface of Fe$_3$O$_4$ particles. Literature data concerning coordination modes of carboxylate group and the metal atom show that in our case, the two oxygen atoms in the carboxylate connected to Fe atoms as a bridging bidentate form [20, 37]. The absorption bands at 583 cm^{-1} in fresh and 571 cm^{-1} in recovered Fe$_3$O$_4$@OA–Pd were attributed to Fe–O stretch vibrations that confirm the existence of Fe$_3$O$_4$ in the two samples. The spectrum of recovered Fe$_3$O$_4$@OA–Pd shows that structural properties of oleic acid to Fe$_3$O$_4$ do not change after completion of the reaction.

Figure 4 shows the FT-IR spectra of the pure Mo$_{10}$V$_2$, fresh Mo$_{10}$V$_2$@NSiO$_2$ and recovered Mo$_{10}$V$_2$@NSiO$_2$. The bands for the Keggin structure of neat Mo$_{10}$V$_2$ occurred at 1096, 1042, 944 and 815 cm^{-1} [30]. The four bands were detected for fresh Mo$_{10}$V$_2$@NSiO$_2$, indicating that the Keggin structure of the Mo$_{10}$V$_2$ was well preserved. The FT-IR spectra of the recovered Mo$_{10}$V$_2$@NSiO$_2$ confirmed that there is no significant change in the structure of the catalyst.
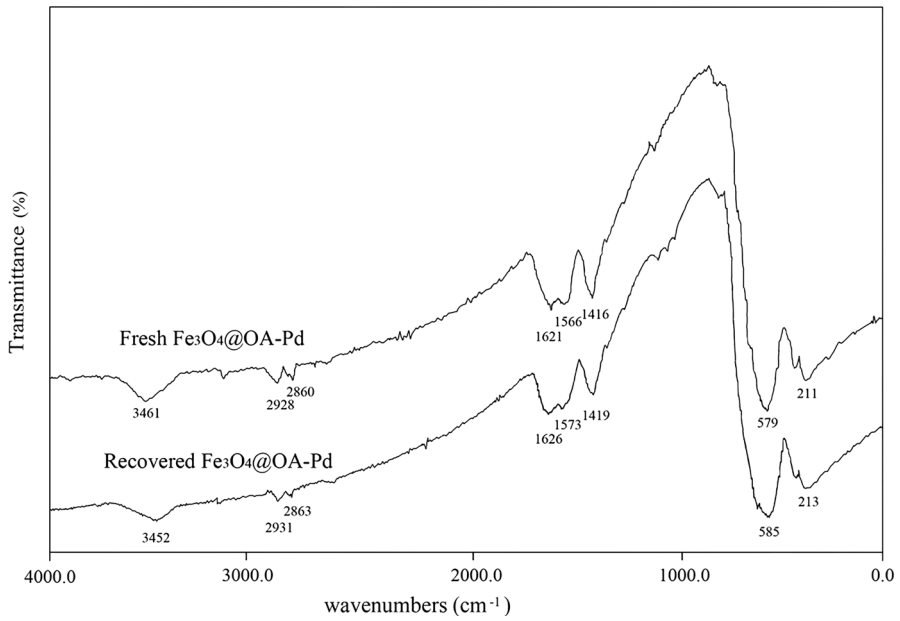
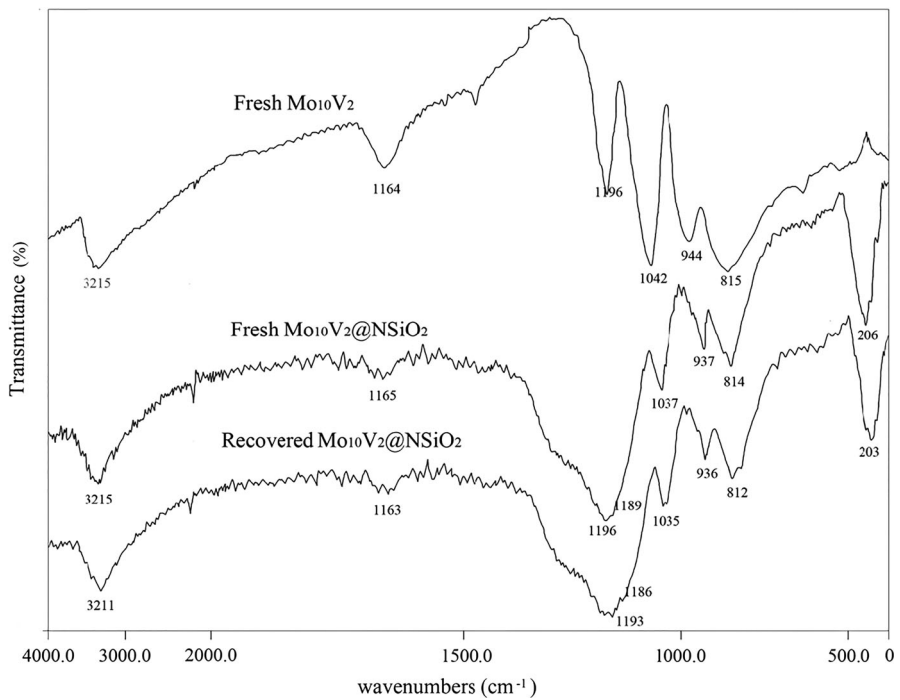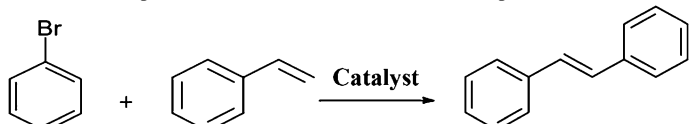**Fig. 3** FT-IR spectra of fresh and recovered Fe_3O_4@OA–Pd

Fig. 4 FT-IR spectra of fresh and recovered $Mo_{10}V_2$@$NSiO_2$ and fresh $Mo_{10}V_2$

The reaction data, along with some literature data for comparison, are given in Table 3. These catalysts showed good reactivity. However, the use of base, ligand and non-recyclable catalysts in these reported systems is not beneficial to industrial and synthetic applications.

Reusability of Fe$_3$O$_4$@OA–Pd and Mo$_{10}$V$_2$@NSiO$_2$ makes the Heck coupling more economical, which encouraged us to study the reusability of this catalytic system in the model reaction. After each run, the desired catalysts were washed with suitable solvent and dried as described in the experimental section. As shown in Fig. 5a, to evaluate the reusability of Mo$_{10}$V$_2$@NSiO$_2$, at the beginning of each run Fe$_3$O$_4$@OA–Pd was used freshly. In the presence of recovered Mo$_{10}$V$_2$@NSiO$_2$, the yield of the product was reduced to an extent of only 15 % from the first run to the third run. Reusability of Fe$_3$O$_4$@OA–Pd was also investigated in the model reaction, as shown in Fig. 5b. It should be noted that to evaluate the recovery of the Fe$_3$O$_4$@OA–Pd at the beginning of each run, Mo$_{10}$V$_2$@NSiO$_2$ was used freshly. The results indicated that Fe$_3$O$_4$@OA–Pd can be recycled three times, albeit with slightly decreasing activity. Finally, synchronized reusability for both components of our catalytic system in the model reaction has been investigated (Fig. 5c) and neither of them were used freshly. The results demonstrate that Fe$_3$O$_4$@OA–Pd and Mo$_{10}$V$_2$@NSiO$_2$ can be simultaneously reused at least three times without apparent loss of their catalytic activity.

A possible mechanism for the Heck reaction in the presence of Fe$_3$O$_4$@OA–Pd and Mo$_{10}$V$_2$@NSiO$_2$ is proposed in Scheme 2. In a first step, the C–X bond of an aryl halide (X = Br, Cl) is oxidatively added to the palladium atom. At this point, the aryl halide bond activation is done by Mo$_{10}$V$_2$@NSiO$_2$ acidic hydrogens. Palladium then forms a π complex with the alkene, and next, the alkene inserts itself in the palladium–carbon bond (Pd–Ar). In the next step, beta-hydride elimination

Table 3 Comparison of the reaction data with other reported methods

Entry	Catalyst	Solvent	Temperature (°C)	Time (h)	Yield (%)	References
1	Pd–Fe$_3$O$_4$	DMF	110	24	76	[38]
2	TiO$_2$@Pd	DMF	140	24	91	[39]
3	Benzimidazolium salt/ Pd(OAc)$_2$	H$_2$O	100	15	71	[40]
4	Pd(II)/[BMIM][TPPMS]	[BMIM][OAc]	140	3	40	[41]
5	Pd(dba)$_2$/P(OPh)$_3$	DMF	100	20	43	[42]
6	Pd (0) MCM-41	DMF	100	24	90	[43]
7	Pd/(SiO$_2$/Fe$_3$O$_4$)	CH$_3$CN/H$_2$O	80–90	12	71	[44]
8	NHC-Pd/SBA-16-IL	NMP	140	40	94	[45]
9	Pd/SiO$_2$	DMA	135	20	90	[46]
11		DMF	120	12	82	This work
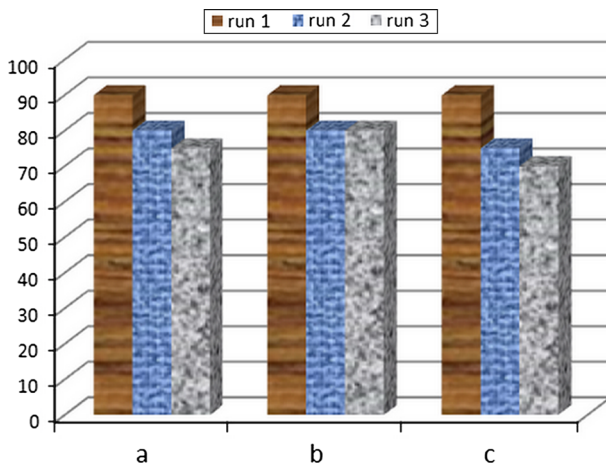
Fig. 5 Reusability of Fe_3O_4@OA–Pd and $Mo_{10}V_2$@$NSiO_2$ in the model reaction (after 8 h). **a** Model reaction with recovered $Mo_{10}V_2$@$NSiO_2$. **b** Model reaction with recovered Fe_3O_4@OA–Pd. **c** Model reaction with recovered $Mo_{10}V_2$@$NSiO_2$ and Fe_3O_4@OA–Pd
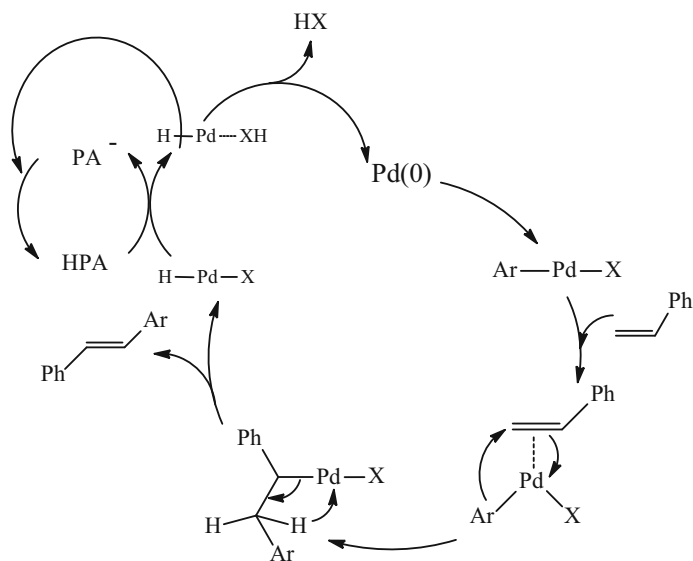
Scheme 2   Proposed mechanism for Heck reaction catalyzed by Fe_3O_4@OA–Pd and $Mo_{10}V_2$@$NSiO_2$

causes formation of a new palladium–alkene π complex. Finally, this complex is destroyed and desired product is released. The palladium(0) compound is regenerated by reductive elimination of the palladium(II) compound using Mo_{10}-V_2@$NSiO_2$. Further research is under investigation in our laboratory.

Conclusion

In conclusion, we have come up with a new stable and heterogeneous catalytic system; Fe$_3$O$_4$@OA–Pd and Mo$_{10}$V$_2$@NSiO$_2$. The present paper reports Heck coupling catalyzed by an efficient ligand and base free heterogeneous catalytic system. The immobilized palladium on oleic acid coated-Fe$_3$O$_4$ was found to be effective in the Heck arylation of various aryl bromides, and especially of less reactive aryl chlorides with styrene in the presence of heteropoly acid. Moreover, the recovery of this system consists of a single filtration for Mo$_{10}$V$_2$@NSiO$_2$ and magnetic separation for Fe$_3$O$_4$@OA–Pd. Both components of this catalytic system are stable under the present reaction conditions, and after separation from reaction media, can be used up to three catalytic cycles without significant loss in activity. Further studies on extending the application of this catalytic system in other organic synthesis are ongoing in our laboratory.

References

1. R.F. Heck, J.P. Nolley, J. Org. Chem. **37**, 2320 (1972)
2. I.P. Beletskaya, A.V. Cheprakov, Chem. Rev. **100**, 3009 (2000)
3. M. Shibasaki, E.M. Vogl, J. Organomet. Chem. **576**, 1 (1999)
4. J. Mo, L. Xu, J. Ruan, S. Liu, J. Xiao, Chem. Commun. 3591 (2006)
5. W.A. Herrmann, C. Brössmer, K. Öfele, C.-P. Reisinger, T. Proermeier, M. Beller, H. Fischer, Angew. Chem. Int. Ed. **34**, 1844 (1995)
6. W.A. Herrmann, V.P.W. Böhm, C.-P. Reisinger, J. Organomet. Chem. **576**, 23 (1999)
7. L. Yin, J. Liebscher, Chem. Rev. **107**, 133 (2007)
8. A. Molnar, Chem. Rev. **111**(3), 2251 (2011)
9. D. Sengupta, J. Saha, G. De, B. Basu, J. Mater. Chem. A **2**, 3986 (2014)
10. B. Basu, S. Das, P. Das, B. Mandal, D. Banerjee, F. Almqvist, Synthesis 1137 (2009)
11. S. Tang, L. Wang, Y. Zhang, S. Li, S. Tian, B. Wang, Fuel Process. Technol. **95**, 84 (2012)
12. B.V. Subba Reddy, A. Siva Krishna, A.V. Ganesh, G.G.K.S. Narayana Kumar, Tetrahedron Lett. **52**, 1359 (2011)
13. R. Parella, N. Srinivasarao, A. Babu, Catal. Commun. **29**, 118 (2012)
14. H.Y. Niu, Z.F. Dizhang, Y.Q.Cai Meng, J. Hazard. Mater. **227**, 195 (2012)
15. H. Liu, Z. Jia, S. Ji, Y. Zheng, M. Li, H. Yang, Catal. Today **175**, 293 (2011)
16. L. Ai, C. Zeng, Q. Wang, Catal. Commun. **14**, 68 (2011)
17. A. Kong, P. Wang, H. Zhang, F. Yang, S. Huang, Y. Shan, Appl. Catal. A: Gen. **183**, 417 (2012)
18. J. Liu, Y. Zhou, F. Liu, C. Liu, J. Wang, Y. Pan, D. Xue, RSC Adv. **2**, 2262 (2012)
19. G. Li, L. Mao, RSC Adv. **2**, 5108 (2012)
20. N. Wu, L. Fu, M. Su, M. Aslam, K.C. Wong, V.P. Dravid, Nano Lett. **4**, 383 (2004)
21. G. Kataby, M. Cojocaru, R. Prozorov, A. Gedanken, Langmuir **15**, 1703 (1999)
22. R. Tadmor, R.E. Rosensweig, J. Frey, J. Klein, Langmuir **16**, 9117 (2000)
23. D. Li, D. Jiang, M. Chen, J. Xie, Y. Wu, S. Dang, J. Zhang, Mater. Lett. **64**, 2462 (2010)
24. K.C. Pereira, A.L. Porter, Sh. Potavathri, A.P. LeBris, B. DeBoef, Tetrahedron **69**, 4429 (2013)
25. A. Corma, S. Iborra, F.X. Llabres i Xamena, R. Monton, J.J. Calvino, C.J. Prestipino, J. Phys. Chem. C. **114**, 8828 (2010)
26. S. Pathan, A. Patel, RSC Adv. **2**, 116 (2012)
27. P. Zhao, Y. Leng, M. Zhang, J. Wang, Y. Wu, J. Huang, Chem. Commun. **48**, 5721 (2012)
28. E. Rafiee, A. Ataei, Sh. Nadri, M. Joshaghani, S. Eavani, Inorg. Chim. Acta **409**, 302 (2014)
29. G.A. Tsigdinos, C.J. Hallada, Inorg. Chem. **7**, 437 (1968)
30. E. Cadot, M. Fournier, A. Teze, G. Herve, Inorg. Chem. **35**, 282 (1996)

31. E. Rafiee, Z. Zolfagharifar, M. Joshaghani, S. Eavani, Appl. Catal. A: Gen. **365**, 287 (2009)
32. E. Rafiee, F. Rahimi, J. Chil. Chem. Soc. **58**, 1926 (2013)
33. Y. Li, Z. Wang, R. Chen, Y. Wang, W. Xing, J. Wang, J. Huang, Catal. Commun. **55**, 34 (2014)
34. T. Jeffery, J.-C. Galland, Tetrahedron Lett. **35**, 4103 (1994)
35. R. Brinkmann, R. Köppler, P. Neiteler, J. Richter, Adv. Mater. **4**, 804 (1992)
36. I. Pryjomska-Ray, A.M. Trzeciak, J.J. Ziolkowski, J. Mol. Catal. A: Chem. **257**, 3 (2006)
37. K. Yang, H. Peng, Y. Wen, N. Li, Appl. Surf. Sci. **256**, 3093 (2010)
38. J. Chung, J. Kim, Y. Jang, S.M. Byun, T. Hyeon, B.M. Kim. Tet. Lett. **54**, 5192 (2013)
39. M. Nasrollahzadeh, A. Azarian, A. Ehsani, M. Khalaj, J. Mol. Catal. A: Chem. **394**, 205 (2014)
40. A. Slamani, S. Demir, I. Özdemir, Catal. Commun. **29**, 141 (2012)
41. Y. Liu, M. Li, Y. Lu, G.H. Gao, Q. Yang, M.Y. He, Catal. Commun. **7**, 985 (2006)
42. J.C. Cárdenas, L. Fadini, C.A. Sierra, Tet. Lett. **51**, 6867 (2010)
43. S. Jana, B. Dutta, R. Bera, S. Koner, Inorg. Chem. **47**, 5512 (2008)
44. Z. Wang, P. Xiao, B. Shen, N. He, Colloids Surf. A **276**, 116 (2006)
45. H. Yang, X. Han, G. Li, Y. Wang, Green Chem. **11**, 1184 (2009)
46. L. Huang, Z. Wang, T.P. Ang, J. Tan, P.K. Wong, Catal. Lett. **112**, 219 (2006)